

Lead glass calorimeter calibration and efficiency analysis for Coulomb sum rule (CSR) experiment in JLab Hall-A

YAN Xihu¹, YE Yunxiu², LYU Haijiang¹,
JIANG Fengjian¹, ZHU Pengjia², SHI Ying¹

(1. Department of Physics, Huangshan University, Huangshan 245041, China;

2. Department of Modern Physics, University of Science and Technology of China, Hefei 230026, China)

Abstract: Two layers of lead glass calorimeter are installed for additional PID analyses in each high resolution spectrometer (HRS) at Hall-A in Jefferson Lab (JLab). The Fumili minimization method of ROOT analysis software and quasi-elastic data of CSR experiment conducted by the authors in the early year of 2008 at JLab were used in the calibration of the calorimeter detector on HRS for the data analysis of CSR experiment. Since some high voltage changes in hardware settings, the lead glass calorimeter detector needed to be calibrated correspondingly. The calibration results are reasonable after this procedure. The best resolution of the calorimeter for the scattering electron was about 0.048 GeV when its momentum was at 1.0 GeV after calibration. Total electron efficiency and pion rejection can reach 99.3% and 99.8%, respectively.

Key words: lead glass calorimeter; resolution; calibration; cut efficiency

CLC number: O572 **Document code:** A doi:10.3969/j.issn.0253-2778.2014.03.009

Citation: Yan Xihu, Ye Yunxiu, Lyu Haijiang, et al. Lead glass calorimeter calibration and efficiency analysis for Coulomb sum rule (CSR) experiment in JLab Hall-A[J]. Journal of University of Science and Technology of China, 2014,44(3):217-220.

JLab Hall-A 上 CSR 实验的铅玻璃量能器刻度与效率分析

闫新虎¹, 叶云秀², 吕海江¹, 蒋峰建¹, 朱鹏佳², 石 瑛¹

(1. 黄山学院物理系, 安徽黄山 245021; 2. 中国科学技术大学近代物理系, 安徽合肥 230026)

摘要: JLab 的 A 大厅里的高分辨谱仪安装了双层的铅玻璃量能器, 用来做粒子鉴别分析. 2008 年初我们在美国的 JLab 获取了全部的 CSR 实验数据, 这里采用了 ROOT 分析软件里的 Fumili 拟合方法和准弹性散射数据对位于高分辨谱仪上的量能器进行刻度. 因为实验过程中硬件高压设置的变化, 需要对 CSR 实验数据进行不同的对应的刻度. 刻度结果表明此刻度修正是合适的. 散射电子动量为 1 GeV 时, 铅玻璃量能器对该能量粒子的最好分辨率为 0.048 GeV. 电子效率和 pion 介子拒绝度可以分别达到 99.3% 和 99.8%.

关键词: 铅玻璃量能器; 分辨率; 刻度; 截断效率

Received: 2013-03-06; **Revised:** 2013-06-10

Foundation item: Supported by the National Natural Science Foundation of China (11135002, 11275083) and Natural Science Foundation of Anhui Education Committee (KJ2012B179, KJ2011B164).

Biography: YAN Xihu (corresponding author), male, born in 1977, PhD. Research field: Medium energy nuclear physics.

E-mail: yanxihu@mail.ustc.edu.cn

0 Introduction

The Coulomb sum rule (CSR)^[1-5] can be defined more explicitly by

$$S_L(q) = \frac{1}{Z} \int_{0^+}^{\infty} \frac{R_L(q, \omega)}{G_E^2} d\omega \quad (1)$$

Eq. (1) was predicted to be unity in the limit of large q , where R_L is the longitudinal response function, $G_E' = (G_E^b + \frac{N}{Z} G_E^n) \zeta$ takes into account the nucleon charge form factor inside the nucleus (which was usually taken to be equal to that of a free nucleon), and ζ is a relativistic correction^[6]. The lower limit of integration 0^+ excludes the elastic peak and the excited states of the nucleus. Z is the number of protons of an atom and ω means energy loss of scattering electron. The CSR can provide some information of nucleon properties in the nuclear medium. To obtain the longitudinal response function R_L , the calibration and efficiency analysis of the lead glass calorimeter detector should be done for the measurement of cross sections of electron scattering off targets.

Two layers of lead glass calorimeter are installed for additional PID analysis in each HRS. The signal detected by lead glass counters is linearly proportional to the energy deposited by the incoming particle^[7]. In JLab Hall A's experiment there are two distributions of energy: low ADC signal for hadrons and high ADC signal for electrons. The limitation on PID efficiency of the lead glass counter comes from separating the tail of the two distributions and hence depends on the energy resolution^[8]. At higher energy the relative resolution of a lead glass counter improves and leads to better separation between the two distributions. A double-layered lead glass calorimeter can provide better separation because the second layer can further separate the hadrons which are contaminated with electrons in the first layer. The two double-layered lead glass calorimeters have different structures on the left and right HRSs.

This article is based on the right HRSs. All lead glass blocks are oriented transversely with respect to the direction of the scattered electrons, as shown in Fig. 1. On the right HRS, the front and second layers of the lead glass counter are called "Preshower" and "Shower" detectors, respectively. The Preshower detector has $2 \times 24 = 48$ blocks of lead glass, $10 \text{ cm} \times 10 \text{ cm} \times 35 \text{ cm}$, oriented transversely with respect to the direction of the scattered electrons. The Shower detector has 5×16 blocks of lead glass, $14.5 \text{ cm} \times 14.5 \text{ cm} \times 35 \text{ cm}$, oriented parallel to the scattered electrons, as shown in Fig. 1. Preshower and Shower together are called "Total Shower" detector. Due to the different thicknesses of the lead glass layers, usually the Total Shower detector on the right HRS has a better PID performance than that of the left HRS. This article will only discuss the calibration and efficiency analysis of lead glass calorimeter in the right HRS.

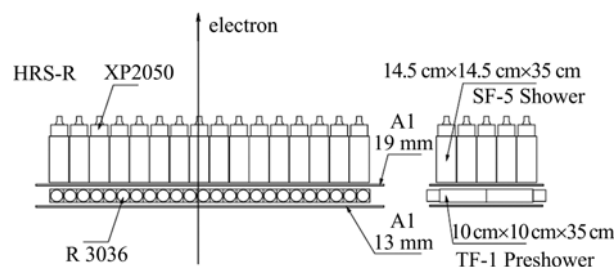


Fig. 1 The schematic of the Preshower and Shower detectors in the right HRS

1 Calibration

As noted in the above section, the Shower detectors are segmented into many individual lead glass blocks, with each block monitored by a single photo-multiplier tube. Since the cascade is in general spread laterally over several adjacent blocks, the outputs are integrated over the entire detector volume to obtain the total detectable signal. When the calorimeter has been calibrated properly, the total deposited energy E will agree with the particle's incident energy or momentum P in the relativistic case.

The calibration method for Preshower and Shower is different from the NaI(Tl) detector of the left HRS since there is no bad block for Preshower and Shower. The calibration constants were obtained with Fumili fitting method^[9], which was used to minimize the Chi-square function as follows:

$$\chi^2 = \sum_{i=1}^n \left[\sum_{j \in M_{ps}^i} C_j \cdot A_j^i + \sum_{k \in M_{sh}^i} C_k \cdot A_k^i - P_{kin}^i \right] \quad (2)$$

where i is the number of selected calibration events; $j(k)$ is the number of Preshower (Shower) block included in the cluster, reconstructed in the i th events; M_{ps}^i is the set of Preshower blocks, included in the cluster; M_{sh}^i is the set of Shower blocks numbers, included in the cluster; A_j^i and A_k^i are the amplitude value in the j th Preshower block and k th Shower block, respectively; P_{kin}^i is the particle momentum; C_j and C_k are the calibration constants to be fitted for the Preshower and Shower, respectively. After the good calibration constants for different HV settings were obtained, a plot of E/p after calibration was obtained as shown in Fig. 2. Since the final peak is actually the sum of all the individual outputs of the phototubes, the width of the peak can provide a measure of how well the detector was calibrated.

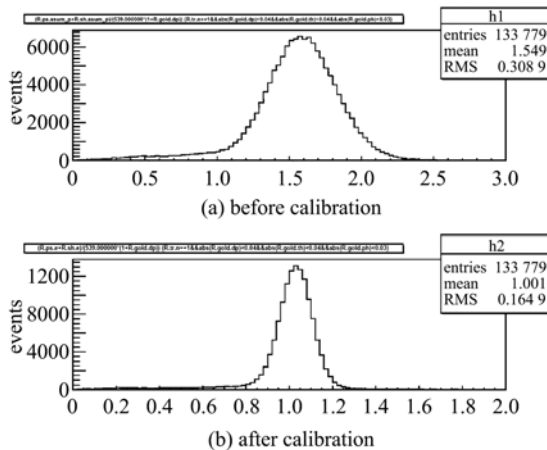


Fig. 2 Preshower and Shower before and after calibration of right HRS (run number 21 884)

We also checked the E/p peak position stability at $E=739$ MeV, $\text{angle}=60^\circ$ as shown in

Fig. 3. From Fig. 3 we can see the E/p peak values are near 1 from 300 MeV to 700 MeV. The maximum deviation is about 2% at 300 MeV. The energy resolution of a calorimeter, expressed in terms of the normalized σ/E , improves with increasing energy.

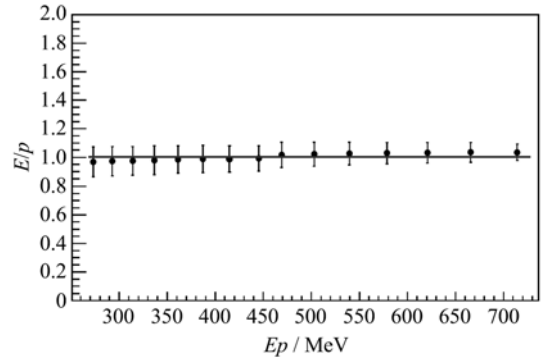


Fig. 3 E/p peak distribution at $E=739$ MeV $\text{angle}=60^\circ$ carbon target

From Fig. 4, we obtained $5.7\%/\sqrt{E}$ at 1 GeV for average resolution of lead glass calorimeter. The best resolution is about $4.8\%/\sqrt{E}$ at 1 GeV and the worst one is about $6\%/\sqrt{E}$ at 1 GeV.

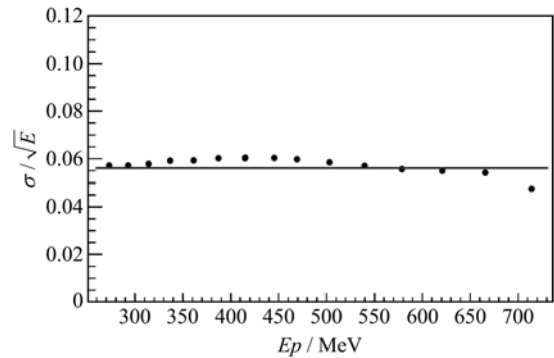


Fig. 4 Resolution of Total Shower at $E=739$ MeV $\text{angle}=60^\circ$ carbon target

2 Detection and cut efficiency

The good electrons are selected from T1 events those with a basic acceptance cut and those that require the Cherenkvo detector to be triggered. We then determine how many of these events also triggered both the Preshower and Shower. The average detection efficiency was better than 99% for almost all runs; A two

dimensional graphical cut on the Preshower and Shower detector was applied to select the good electrons and exclude low energy “junk” events and pions as shown in Fig. 5.

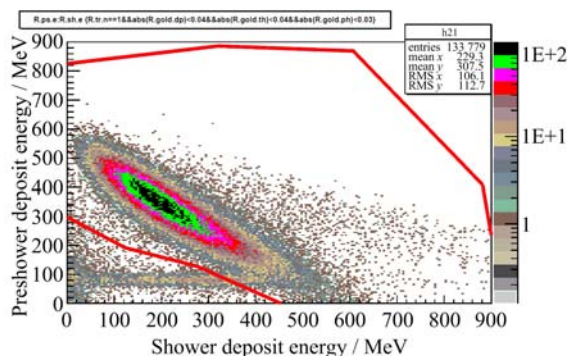


Fig. 5 The graphic cut efficiency of the scattering electrons for the Preshower and Shower at $E=539$ MeV, angle= 60°

The choice of a graphical cut was made so that the pion suppression is large while the total number of good events excluded by the graphical cut was always less than 1%. The graphical cut efficiency for electron and pion rejection in Fig. 5 is 99.6% and 78.9%, respectively.

3 Conclusion

The Hall-A HRS lead glass calorimeters had been calibrated throughout the CSR experiment. The reliable calibration constants were obtained. The $E=p$ plots for all runs with the corresponding constants were reasonable, the peak for all runs were close to 1, indicating that the calibration was successful. The best resolution of the calorimeter on Hall-A right HRS for the scattering electron was about 0.048 GeV when its momentum was 1.0 GeV. Finally, we combined the Cherenkov and Total Shower PID cuts together, and obtained total electron efficiency

$$\epsilon_e^- = 0.997 \times 0.996 = 0.993 (\text{i. e. } 99.3\%)$$

and pion rejection

$$\epsilon_{\pi^-} = 1 - (1 - 0.991) \times (1 - 0.789) = 0.998 (\text{i. e. } 99.8\%).$$

Knowledgegments I would like to thank Chen J P for his suggestion and Sulkosky V, Alexandre C for their advices.

References

- [1] Chen J P, Meziani Z E, Beck D, et al. Longitudinal and transverse response functions in $^{56}\text{Fe}(e, e')$ at momentum transfer near 1 GeV/c[J]. Phys Rev Lett, 1991, 66: 1 283-1 286.
- [2] Meziani Z E, Barreau P, Bernheim M, et al. Coulomb sum rule for ^{40}Ca , ^{48}Ca , and ^{56}Fe for $|\mathbf{q}| \leq 500$ MeV/c[J]. Phys Rev Lett, 1984, 52: 2 130-2 133.
- [3] Meziani Z E, Barreau P, Bernheim M, et al. Transverse response functions in deep-inelastic electron scattering for ^{40}Ca , ^{48}Ca , and ^{56}Fe [J]. Phys Rev Lett, 1985, 54: 1 233-1 236.
- [4] Deady M, Williamson C F, Zimmerman P D, et al. Deep inelastic separated response functions from ^{40}Ca and ^{48}Ca [J]. Phys Rev C, 1986, 33: 1 897-1 904.
- [5] Blatchley C C, LeRose J J, Pruet O E, et al. Quasi-elastic electron scattering from ^{238}U [J]. Phys Rev C, 1986, 34: 1 234-1 247.
- [6] De Forest Jr T. The relativistic Coulomb sum rule for electron scattering in the independent-particle model [J]. Nucl Phys A, 1984, 414(3): 347-358.
- [7] Grupen C. Particle Detectors [M]. Cambridge: Cambridge University Press, 1996: 193.
- [8] Liyanage N. A study of the $^{16}\text{O}(e, e'p)$ reaction at deep missing energies[D]. Massachusetts Institute of Technology, Cambridge, Massachusetts, 1999.
- [9] Alcorn J, et al (JLab Collaboration). Basic instrumentaion for Hall A at Jefferson Lab[J]. Nuclear Instruments and Methods in Physics Research A, 2004, 522: 294-346.